

## Theoretical Study of the Methylbenzene Side-Chain Hydrocarbon Pool Mechanism in Methanol to Olefin Catalysis

Bjørnar Arstad,<sup>†</sup> John B. Nicholas, and James F. Haw\*

Contribution from the Department of Chemistry, University of Southern California, University Park, Los Angeles, California 90089

Received May 2, 2003; Revised Manuscript Received October 22, 2003; E-mail: jhaw@usc.edu

**Abstract:** Recent experimental work has shown that methanol to olefin (MTO) catalysis on microporous solid acids proceeds through a hydrocarbon pool mechanism with methylbenzenes frequently acting as the most important reaction centers. Other recent experimental evidence suggests that side-chain methylation is more important than an alternative paring (ring contraction–expansion) mechanism. The present investigation uses density functional theory B3LYP/cc-pVTZ//B3LYP/6-311G\* and G3(MP2) calculations to model many of the features of the side-chain mechanism. We first calculated at the G3(MP2) level the heats of formation of 43 neutral alkylbenzenes to predict the thermodynamics for methylation reactions. The G3(MP2) results predict that sequential methylation of benzene rings with fewer than four methyl groups will preferentially occur on the ring, resulting in the series toluene, 1,3-dimethylbenzene, 1,2,4-trimethylbenzene, and 1,2,4,5-tetramethylbenzene. With the addition of another methyl group side-chain methylation becomes preferred, with 1-ethyl-2,4,5-tetramethylbenzene predicted to be more stable than pentamethylbenzene by 0.7 kcal/mol. We modeled the entire gas-phase side-chain reaction mechanism at the B3LYP/cc-pVTZ//B3LYP/6-311G\* level, using *p*-xylene, 1,2,3,5-tetramethylbenzene, and hexamethylbenzene as reaction centers and following the reaction to the point of producing both ethylene and propene. B3LYP/6-311G\* analytical frequencies were calculated in order to obtain the data needed for the prediction of enthalpies. For comparison, G3(MP2) enthalpies were also calculated for the mechanism based on *p*-xylene only. We also used a zeolite cluster model to more accurately describe the relative energetics of the reaction for the entire hexamethylbenzene mechanism and parts of the *p*-xylene mechanism. These calculations place the side-chain mechanism on a much stronger foundation and reproduce experimental structure–reactivity and structure–selectivity data for the methylbenzene hydrocarbon pool.

### Introduction

The conversion of methanol to olefins (MTO) or other hydrocarbons<sup>1–3</sup> on microporous solid acids is a key step in the synthesis of polyolefins from methane. The mechanism of MTO catalysis has been a long-standing academic problem, and there were at least 20 distinct proposals for this chemistry that embrace almost every type of reactive intermediate.<sup>4</sup> A series of papers from the Kolboe<sup>5–9</sup> and Haw<sup>10–15</sup> groups have settled

this issue in favor of some type of hydrocarbon pool mechanism. In our recent Communication in this journal we showed that methanol has little or no reactivity on two important MTO catalysts if great care is taken to remove organic impurities that form the primordial hydrocarbon pool and initiate the reaction.<sup>16</sup> This finding is especially strong evidence for a hydrocarbon pool mechanism in MTO chemistry.

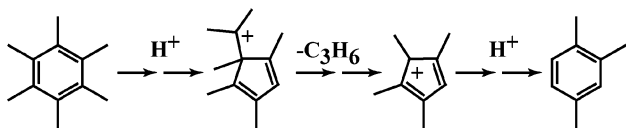
Within the hydrocarbon pool hypothesis it is possible to imagine many detailed mechanisms involving various organic reaction centers (the active hydrocarbon pool species) that take part in catalytic cycles. Many of these pathways can be tested experimentally. Known hydrocarbon pool species include methylbenzenes,<sup>12</sup> methyl-naphthalenes,<sup>13</sup> methylcyclopentenyl cations,<sup>12</sup> and in some cases simple olefins. There are two long-standing explanations of how methylbenzenes function as hydrocarbon pool species.

<sup>†</sup> Present address: Department of Chemistry, University of Oslo, P.O. Box 1033 Blindern, N-0315 Oslo, Norway.

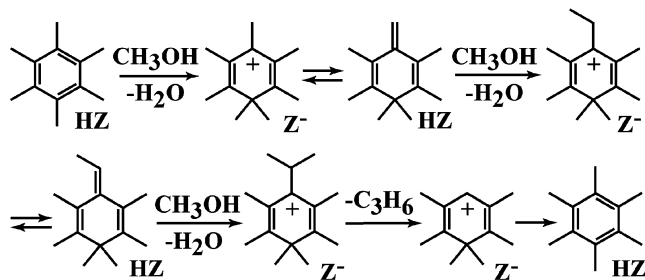
- (1) Chang, C. D. *Catal. Rev.* **1983**, *25*, 1–118.
- (2) Chang, C. D. *Shape-Selective Catalysis: Chemicals Synthesis and Hydrocarbon Processing*; Song, C., Garces, J. M., Sugi, Y., Ed.; ACS Symposium Series 738; Washington D.C., 2000.
- (3) Haw, J. F.; Song, W.; Marcus, D. M.; Nicholas, J. B. *Acc. Chem. Res.* **2003**, *36*, 317–326.
- (4) Stöcker, M. *Microporous Mesoporous Mater.* **1999**, *29*, 3–48.
- (5) Dahl, I. M.; Kolboe, S. J. *Catal.* **1994**, *149*, 458–464.
- (6) Dahl, I. M.; Kolboe, S. J. *Catal.* **1996**, *161*, 304–309.
- (7) Mikkelsen, O.; Ronning, P. O.; Kolboe, S. *Microporous Mesoporous Mater.* **2000**, *40*, 95–113.
- (8) Arstad, B.; Kolboe, S. *Catal. Lett.* **2001**, *71*, 209–212.
- (9) Arstad, B.; Kolboe, S. *J. Am. Chem. Soc.* **2001**, *123*, 8137–8138.
- (10) Goguen, P. W.; Xu, T.; Barich, D. H.; Skloss, T. W.; Song, W.; Wang, Z.; Nicholas, J. B.; Haw, J. F. *J. Am. Chem. Soc.* **1998**, *120*, 2651–2652.
- (11) Haw, J. F.; Nicholas, J. B.; Song, W.; Deng, F.; Wang, Z.; Heneghan, C. S. *J. Am. Chem. Soc.* **2000**, *122*, 4763–4775.

- (12) Song, W.; Haw, J. F.; Nicholas, J. B.; Heneghan, K. *J. Am. Chem. Soc.* **2000**, *122*, 10726–10727.
- (13) Song, W.; Fu, H.; Haw, J. F. *J. Phys. Chem. B* **2001**, *105*, 12839–12843.
- (14) Song, W.; Fu, H.; Haw, J. F. *J. Am. Chem. Soc.* **2001**, *123*, 4749–4754.
- (15) Sassi, A.; Wildman, M.; Ahn, H. J.; Prasad, P.; Nicholas, J. B.; Haw, J. F. *J. Phys. Chem. B* **2002**, *106*, 2294–2303.
- (16) Song, W.; Marcus, D. M.; Fu, H.; Ehresmann, J. O.; Haw, J. F. *J. Am. Chem. Soc.* **2002**, *124*, 3844–3845.

Scheme 1



Scheme 2



The paring reaction was proposed in 1961 to account for the conversion of hexamethylbenzene to isobutane and other products on a bifunctional catalyst in a hydrogen gas stream.<sup>17</sup> In the paring mechanism of MTO catalysis a benzenium cation ring contracts from six carbons to five carbons, and then expands back to six, such that an alkyl chain is extended in the process. As in other hydrocarbon pool mechanisms this alkyl chain would be eliminated as an olefin on an MTO catalyst. Scheme 1 shows one highly simplified way to think of the paring route (there are obviously others that could be drawn).

Carbon label scrambling between ring and methyl positions is possible evidence of the paring mechanism. While scrambling is frequently observed,<sup>9,15</sup> its mechanistic significance is so far not certain. Ring expansion and contraction by a benzyl-tropylium type route has been suggested as an alternative explanation for label scrambling.<sup>15</sup> The second explanation for the involvement of methylbenzenes as hydrocarbon pool species was put forth by Mole and co-workers, who were the first to propose side-chain methylation of methylbenzenes during MTO catalysis.<sup>18</sup> This mechanism was devised to account for a “cocatalytic” effect of toluene in methanol conversion catalysis on zeolite HZSM-5. Scheme 2 shows our re-interpretation of Mole’s original mechanism.

Our schemes<sup>15</sup> show cation formation by *gem*-dimethylation of aromatic rings, rather than by protonation, as in the original source literature.<sup>18</sup> There is experimental evidence for *gem*-dimethyl benzenium cations as persistent species in zeolites. For example, a pentamethylbenzenium cation has been observed in HZSM-5<sup>19</sup> whereas the heptamethylbenzenium cation has been observed in zeolite HBeta by in situ NMR.<sup>20</sup> Zeolites are not sufficiently strong acids to form a persistent benzenium ion by protonation,<sup>21–24</sup> and all of our theoretical work to date shows

that protonated benzene rings in zeolites transfer the proton back to the catalyst without a barrier. In contrast we find barriers for the loss of the  $\text{CH}_3^+$  group. A key feature of the side-chain mechanism of MTO catalysis is deprotonation of a benzenium cation side chain to form an exocyclic olefin (Scheme 2). Methylation of the exocyclic double bond leads successively to ethyl or (iso)propyl groups that are liberated as the corresponding olefins; Scheme 2 shows the specific case of an isopropyl group forming propene.

In the paring mechanism hexamethylbenzene could react, for example, to form propene and trimethylbenzene, and the starting material would be regenerated by subsequent ring methylation. In the side-chain mechanism, methylation would occur directly onto one of the side chains of hexamethylbenzene or another methylbenzene. We recently tested which mechanism is most important by directly pulsing methylbenzenes and other reactants onto the large pore zeolite HBeta.<sup>15</sup> A pulse consisting of hexamethylbenzene and 5 equiv of water produced very low levels of olefins. In contrast, a pulse of toluene and 5 equiv of methanol showed very high conversion to olefins. These two pulses would result in the same stoichiometry if ring methylation were more important than side-chain methylation. Rather, after a small fraction of the toluene was ring methylated the resulting methylbenzenes apparently became active for the side-chain mechanism, and the remainder of the methanol was converted to olefins on these.

In this investigation we used theoretical calculations to put some features of the side-chain mechanism on a more solid footing. Our objectives included determining why methylbenzenes with five or six methyl groups are much more active as reaction centers than those with fewer methyl groups, as well as why the propene/ethylene product selectivity ratio increases with the number of methyl groups on the benzene ring. We used the G3(MP2) level of theory to predict the thermodynamics of ring and side-chain methylation reactions on a variety of methyl-substituted benzenes. We used the B3LYP/6-311G\* and B3LYP/cc-pVTZ//B3LYP/6-311G\* levels of theory to model gas-phase side-chain mechanisms from methanol to ethylene or propene starting from *p*-xylene, two routes based on 1,2,3,5-tetramethylbenzene, and hexamethylbenzene. We optimized minima (reactants, products, and intermediates) only. For the single, more tractable case of *p*-xylene, we repeated all of the calculations using the G3(MP2) level of theory to estimate the accuracy of the B3LYP/cc-pVTZ//B3LYP/6-311G\* data. The highest energy intermediate on the G3(MP2) potential surface is 9.4 kcal/mol lower in enthalpy relative to the same species on the B3LYP/cc-pVTZ//B3LYP/6-311G\* surface; therefore, the plausibility of the mechanism is improved by consideration of the more accurate calculations. We repeated all of the B3LYP/cc-pVTZ//B3LYP/6-311G\* energy calculations for the hexamethylbenzene mechanism and several key points for the *p*-xylene mechanism with the organic species in contact with an  $(\text{H}_3\text{SiO})_3\text{SiOHAl}(\text{OSiH}_3)_3$  model of the zeolite acid site. These calculations corrected the artificially low energies of several protonated species that are obtained using  $\text{H}^+$  to model the acid site in the gas-phase calculations.

The overall results of the study strongly support the methylbenzene side-chain mechanism in MTO catalysis. The G3(MP2) calculations provided some surprising results on the thermodynamic stabilities of various alkylbenzene isomers. Methylation

(17) Sullivan, R. F.; Egan, C. J.; Langlois, G. E.; Sieg, R. P. *J. Am. Chem. Soc.* **1961**, *83*, 1156–1160.

(18) Mole, T.; Whiteside, J. A.; Seddon, D. *J. Catal.* **1983**, *82*, 261–266.

(19) Xu, T.; Barich, D. H.; Goguen, P. W.; Song, W.; Wang, Z.; Nicholas, J. B.; Haw, J. F. *J. Am. Chem. Soc.* **1998**, *120*, 4025–4026.

(20) Song, W.; Nicholas, J. B.; Sassi, A.; Haw, J. F. *Catal. Lett.* **2002**, *81*, 49–53.

(21) Haw, J. F.; Nicholas, J. B.; Xu, T.; Beck, L. W.; Ferguson, D. B. *Acc. Chem. Res.* **1996**, *29*, 259–267.

(22) Arstad, B.; Kolboe, S.; Swang, O. *J. Phys. Chem. B.* **2002**, *106*, 12722–12726.

(23) Beck, L. W.; Xu, T.; Nicholas, J. B.; Haw, J. F. *J. Am. Chem. Soc.* **1995**, *117*, 11594–11595.

(24) Xu, T.; Barich, D. H.; Torres, P. D.; Haw, J. F. *J. Am. Chem. Soc.* **1997**, *119*, 406–414.

of toluene, xylene, and trimethylbenzene is always preferred on ring versus side-chain positions. But for tetramethylbenzene the enthalpy changes for side-chain and ring methylation were nearly identical, and for pentamethylbenzene side-chain methylation is preferred by ca. 2 kcal/mol. To the extent that the relative energies of intermediates in the formation of ethylene and propene are predictive of the relative barriers, the B3LYP/cc-pVTZ//B3LYP/6-311G\* enthalpies clearly reproduce experimentally deduced relationships between the number of methyl groups and activity and selectivity.

## Theoretical Methods

We initially used density functional theory<sup>25</sup> at the B3LYP/6-311G\* level<sup>26,27</sup> to optimize the geometries of a large number of methyl- and alkylbenzene isomers in order to study the relative energetics of ring versus side-chain alkylation. We also optimized all species along the gas-phase reaction pathways (minima only) for the conversion of methanol to ethylene or propene on *p*-xylene, 1,2,3,5-tetramethylbenzene (two pathways), and hexamethylbenzene reaction centers. Analytical frequency calculations were used to verify the geometries as minima and to obtain the zero-point and thermal energy corrections needed to predict reaction enthalpies. As expected, the B3LYP/6-311G\* level of theory is not able to provide highly accurate thermochemical data, especially for nonisodesmic reactions such as breaking C–O bonds and forming C–C bonds in their place. For example, the B3LYP/6-311G\* enthalpy for the gas-phase reaction 2 methanol → ethylene + 2H<sub>2</sub>O is +7.6 kcal/mol, whereas the experimental enthalpy change<sup>28,29</sup> is –7.06 kcal/mol. Similarly, the predicted B3LYP/6-311G\* reaction enthalpy for 3 methanol → propene + 3H<sub>2</sub>O is –2.4 kcal/mol, whereas the experimental enthalpy change is –24.52 kcal/mol. To address this energetic deficiency, we obtained more accurate single-point energies at the B3LYP/cc-pVTZ//B3LYP/6-311G\* level of theory<sup>30</sup> with the basis sets augmented to include diffuse functions on oxygen. At this level, the above reaction enthalpies are predicted to be –5.6 kcal/mol and –20.8 kcal/mol, a substantial improvement. This level of theory was tractable for all the species we wished to study, even when we also included a zeolite cluster model.

To obtain even more accurate data we also used Gaussian-3 theory with reduced Møller–Plesset order, G3(MP2),<sup>31</sup> to calculate the standard enthalpies of formation of a total of 57 compounds (as well as benzene and toluene, which were previously reported), including every minimum-energy structure on the reaction pathway for converting methanol to ethylene or propene on a *p*-xylene reaction center in the gas phase (i.e., without a zeolite cluster). For the 222 compounds in the G3/99 test set the mean absolute deviation from the experimental enthalpy of formation is 1.22 kcal/mol, which decreases to 0.71 kcal/mol for the 38 hydrocarbons in that set. Unfortunately, the only aromatic hydrocarbons in that set are benzene and toluene. The computationally most demanding step in G3(MP2) theory is a single-point energy calculation at the QCISD(T) level. At the G3(MP2) level, the above-mentioned reaction enthalpies are predicted to be –7.64 kcal/mol and –24.97, giving an even better agreement with experiment than the B3LYP/cc-pVTZ//B3LYP/6-311G\* calculations.

In the gas-phase reaction mechanism calculations, we simply used H<sup>+</sup> to represent the zeolite acid. To more accurately study the effects

of the zeolite acid site we also calculated the pathway for converting hexamethylbenzene to ethylene and propene as well as several key points for the reaction on *p*-xylene using a (H<sub>3</sub>SiO)<sub>3</sub>SiOHAl(OSiH<sub>3</sub>)<sub>3</sub> cluster model that we have previously used in related work.<sup>21</sup> Our zeolite model is based on the X-ray crystal structure of a site in zeolite HZSM-5, but its properties would not be appreciably different from that of other aluminosilicate zeolites. In all the optimizations the terminal silyl (H<sub>3</sub>Si-) groups were held fixed in crystallographic positions corresponding to the T(12)–O(24)–T(12) site in HZSM-5.<sup>32</sup> The positions of all other atoms were allowed complete freedom. The constraints imposed in the optimizations preclude the calculation of thermodynamic properties, we thus report changes in energy ( $\Delta E$ ) rather than enthalpy for the cluster calculations. All calculations presented in this contribution were performed using Gaussian 98.<sup>33</sup>

## Results

**Energetics of Ring and Side-Chain Alkylation.** Our own experimental work showed that pentamethylbenzene and hexamethylbenzene were far more active for MTO catalysis than, for example, xylenes.<sup>14,15</sup> We thus considered the possibility that the thermochemical penalties for side-chain methylation would decrease with additional methyl groups on the ring. Experimental gas-phase enthalpies of formation are available for all methylbenzene isomers, but for very few benzene derivatives with one or more methyl groups and an alkyl chain. Thus, on the basis of experimental thermochemical data for neutral molecules it is difficult to assess the reasonableness of either route. To supplement the experimental data we used the G3(MP2) method,<sup>31</sup> the most accurate model chemistry tractable for the hydrocarbons under study. Our results are reported in Table 1 and are compared to experimental values of the gas-phase enthalpy of formation where available.<sup>28,29</sup> The agreement between computed and experimental values is generally excellent. The average absolute deviation for 20 aromatic hydrocarbons not previously reported at the G3(MP2) level is 1.63 kcal/mol. All the deviations from experimental results are in same direction, toward more negative  $\Delta H$ 's.

One way to test the reasonableness of side chain versus ring methylation reactions is to compare the difference in the enthalpy of formation between the appropriate species. For example, *m*-xylene (the experimentally lowest energy xylene) is 3.00 kcal/mol (experiment) or 2.5 kcal/mol (G3(MP2)) more stable than ethylbenzene, and on this basis alone we should not expect toluene to preferentially undergo side-chain methylation. We would predict that methylation of the most stable xylene (*m*-xylene) would preferentially lead to 1,2,4-trimethylbenzene rather than to the less stable 1-ethyl-4-methylbenzene. Thus, in the gas phase the overall reaction *m*-xylene + methanol → 1,2,4-trimethylbenzene + H<sub>2</sub>O is exothermic by –17.3 kcal/mol whereas the reaction *m*-xylene + methanol → 1-ethyl-4-methylbenzene + H<sub>2</sub>O is less exothermic at –14.7 kcal/mol.

- (25) Parr, R. G.; Yang, W. *Density-Functional Theory of Atoms and Molecules*; Oxford University Press: 1994.
- (26) Becke, A. D. *J. Chem. Phys.* **1993**, *98*, 5648–5652.
- (27) Hehre, W. J.; Radom, L.; Schleyer, P. v. R.; Pople, J. A. *Ab Initio Molecular Orbital Theory*; John Wiley & Sons: New York, 1986.
- (28) NIST Chemistry WebBook (<http://webbook.nist.gov/chemistry/>).
- (29) Chase, M. W., Jr. NIST-JANAF Thermochemical Tables, *J. Phys. Chem. Ref. Data*, Monograph 9, **1998**.
- (30) Kendall, R. A.; Dunning, T. H., Jr.; Harrison, R. J. *J. Chem. Phys.* **1992**, *96*, 6796–6806.
- (31) Curtiss, L. A.; Raghavachari, K.; Redfern, P. C.; Rassolov, V.; Pople, J. A. *J. Chem. Phys.* **1998**, *109*, 7764–7776.

(32) van Koningsveld, H.; van Bekkum, H.; Jansen, J. C. *Acta Crystallogr.* **1987**, *B43*, 127–132.

(33) Frisch, M. J.; Trucks, G. W.; Schlegel, H. B.; Scuseria, G. E.; Robb, M. A.; Cheeseman, J. R.; Zakrzewski, V. G.; Montgomery, J. A., Jr.; Stratmann, R. E.; Burant, J. C.; Dapprich, S.; Millam, J. M.; Daniels, A. D.; Kudin, K. N.; Strain, M. C.; Farkas, O.; Tomasi, J.; Barone, V.; Cossi, M.; Cammi, R.; Mennucci, B.; Pomelli, C.; Adamo, C.; Clifford, S.; Ochterski, J.; Petersson, G. A.; Ayala, P. Y.; Cui, Q.; Morokuma, K.; Salvador, P.; Dannenberg, J. J.; Malick, D. K.; Rabuck, A. D.; Raghavachari, K.; Foresman, J. B.; Cioslowski, J.; Ortiz, J. V.; Baboul, A. G.; Stefanov, B. B.; Liu, G.; Liashenko, A.; Piskorz, P.; Komaromi, I.; Gomperts, R.; Martin, R. L.; Fox, D. J.; Keith, T.; Al-Laham, M. A.; Peng, C. Y.; Nanayakkara, A.; Challacombe, M.; Gill, P. M. W.; Johnson, B.; Chen, W.; Wong, M. W.; Andres, J. L.; Gonzalez, C.; Head-Gordon, M.; Replogle, E. S.; Pople, J. A. *Gaussian 98*, Revision A.10; Gaussian, Inc.: Pittsburgh, PA, 2001.



**Table 1.** G3(MP2) Enthalpies of Formation (Calculated at 298.15 K) for Aromatic Hydrocarbons, Cyclic Trienes with an Exocyclic Double Bond, Methanol, Water, Ethylene, and Propene, Compared with Experimental (Gas-Phase) Values Where Available<sup>a</sup>

molecule	exptl	G3(MP2)
<b>C<sub>8</sub>H<sub>10</sub></b>		
<i>o</i> -xylene	4.54	2.77
<i>m</i> -xylene	4.12	3.00
<i>p</i> -xylene	4.29	3.15
ethylbenzene	7.12	5.50
<b>C<sub>9</sub>H<sub>12</sub></b>		
1,2,4-trimethylbenzene	-3.33	-4.89
1,3,5-trimethylbenzene		-4.81
1,2,3-trimethylbenzene	-2.29	-3.88
1-ethyl-2-methylbenzene	+0.29	-1.93
1-ethyl-3-methylbenzene	-0.46	-2.31
1-ethyl-4-methylbenzene	-0.78	-2.17
<i>n</i> -propylbenzene	+1.87	+0.10
isopropylbenzene	+0.94	-1.00
6-methylene-3,3-dimethyl-cyclohexa-1,4-diene		+23.65
<b>C<sub>10</sub>H<sub>14</sub></b>		
1,2,3,4-tetramethylbenzene	-8.61	-10.41
1,2,3,5-tetramethylbenzene	-10.33	-11.51
1,2,4,5-tetramethylbenzene	-11.3	-12.85
1-ethyl-2,3-dimethylbenzene		-8.88
1-ethyl-2,4-dimethylbenzene		-9.65
1-ethyl-2,5-dimethylbenzene		-9.63
1-ethyl-2,6-dimethylbenzene		-9.01
1-ethyl-3,4-dimethylbenzene		-10.25
1-ethyl-3,5-dimethylbenzene		-10.09
1- <i>n</i> -propyl-2-methylbenzene		-7.45
1- <i>n</i> -propyl-3-methylbenzene		-7.71
1- <i>n</i> -propyl-4-methylbenzene		-7.56
1-isopropyl-2-methylbenzene		-7.64
1-isopropyl-3-methylbenzene		-8.84
1-isopropyl-4-methylbenzene		-8.67
<i>n</i> -butylbenzene	-3.30	-5.05
<i>sec</i> -butylbenzene	-4.17	-5.78
isobutylbenzene	-5.15	-7.36
<i>tert</i> -butylbenzene	-5.42	-7.69
<b>C<sub>11</sub>H<sub>16</sub></b>		
pentamethylbenzene	-16.1	-16.89
1-ethyl-2,4,5-trimethylbenzene		-17.62
1-ethyl-3,4,5-trimethylbenzene		-16.84
1- <i>n</i> -propyl-2,6-dimethylbenzene		-14.61
1- <i>n</i> -propyl-3,5-dimethylbenzene		-15.52
1-isopropyl-3,5-dimethylbenzene		-16.65
6-isopropylidene-3,3-dimethyl-cyclohexa-1,4-diene		+11.19
<b>C<sub>12</sub>H<sub>18</sub></b>		
hexamethylbenzene	-18.5	-19.92
1-ethyl-2,3,5,6-tetramethylbenzene		-22.00
1- <i>n</i> -propyl-2,4,5-trimethylbenzene		-22.98
1- <i>n</i> -propyl-2,4,6-trimethylbenzene		-22.14
1-isopropyl-3,4,5-trimethylbenzene		-23.45
<b>C<sub>13</sub>H<sub>20</sub></b>		
1-ethyl-2,3,4,5,6-pentamethylbenzene		-25.33
methanol	-48.0	-47.66
water	-57.80	-57.41
ethylene	12.54	11.86
propene	4.88	4.28

<sup>a</sup> All values reported in kcal/mol.

Following this line of reasoning, the first reaction for which side-chain methylation is preferred is the formation of 1-ethyl-2,4,5-trimethylbenzene by methylation of 1,2,4,5-tetramethylbenzene. In the gas phase the overall reaction 1,2,4,5-tetramethylbenzene + methanol → 1-ethyl-2,4,5-trimethylbenzene + H<sub>2</sub>O is predicted to be exothermic by -14.5 kcal/mol. For the next larger series the most favorable overall gas-phase reaction is pentamethylbenzene + methanol → 1-ethyl-2,3,5,6-tetramethylbenzene + H<sub>2</sub>O, predicted to be exothermic by

-14.9 kcal/mol. The gas-phase reaction hexamethylbenzene + methanol → 1-ethyl-2,3,4,5,6-pentamethylbenzene + H<sub>2</sub>O is predicted to be exothermic by -15.2 kcal/mol. This is even more exothermic than methylation of pentamethylbenzene to hexamethylbenzene (-12.8 kcal/mol). Further methylation of ethylpentamethylbenzene to isopropylpentamethylbenzene is also quite exothermic on the basis of calculations at lower levels of theory (not shown). The results in Table 1 show that formation of an alkyl chain on a benzene ring with a large number of methyl group substituents is thermodynamically favorable.

#### Proposed Side-Chain Reaction Mechanism for *p*-Xylene.

Our starting point for modeling the side-chain routes on methylbenzene reaction centers was our recent theoretical study of the very similar reactions of dimethylcyclopentenyl carbenium ion reaction centers in zeolite HZSM-5.<sup>10</sup> These cyclic carbenium ions form very readily in acidic zeolites from a variety of precursors, and they clearly can function in hydrocarbon pool mechanisms. At higher temperatures, the dimethylcyclopentenyl carbenium ion is converted into toluene, which is also a cocatalyst in MTO chemistry. The scheme in Figure 1 shows the minimum-energy species (reactants, intermediates, and products) along a gas-phase surface taking *p*-xylene (the reaction center) and three methanol molecules to either ethylene or propene with regeneration of *p*-xylene. Each step entails either a (de)protonation, a (de)methylation, or the elimination of an olefin. In ref 10 we theoretically modeled the transition states for the analogous reactions in the cyclopentenyl system. We did not attempt transition state calculations in this work. Also, in Figure 1, as well as the other gas-phase reaction schemes presented in Figures 2–4, the acidic zeolite is represented as only a proton. Thus, we are not accounting for the energy required to remove the proton from the zeolite (the zeolite proton affinity) nor the resulting ionic attraction between the anionic zeolite conjugate base and the cationic hydrocarbon. Consequently, all of the gas-phase schemes show large relative energy differences between neutral and cationic species. As mentioned earlier for the specific case of hexamethylbenzene (vide infra, Figure 6), we included a cluster model of the zeolite acid site in the calculations, and as will be seen, this results in a much more reasonable appearance for the potential surface.

The first step of the reaction presented in Figure 1 is the methylation of *p*-xylene. There are two possible isomers resulting: the 1,2,4-trimethylbenzenium cation and the 1,1,4-trimethylbenzenium cation. A key feature of all of our proposed reaction mechanisms is the formation of a species in which *gem*-dimethylation occurs in a position *ortho* or *para* to a methyl or ethyl substituent. If the reaction produces the 1,2,4-trimethylbenzenium cation, we predict that it will simply lose a proton to generate 1,2,4-trimethylbenzene. This is keeping with our prediction that only a few highly substituted cations (with parent olefins or aromatics having a proton affinity of ~209 kcal/mol or greater) are persistent in acidic zeolites.<sup>34</sup> Cations formed from slightly less basic hydrocarbons can surely have a transient existence, but the less basic the parent hydrocarbon, the less reasonable is its protonated form. For example, 1,2,4-trimethylbenzene is not very basic (proton affinity = 190.8 kcal/mol), and the corresponding cation will readily give a proton back to the zeolite. Ring methylation does not directly lead to

(34) Nicholas, J. B.; Haw, J. F. *J. Am. Chem. Soc.* **1998**, *120*, 11804–11805.

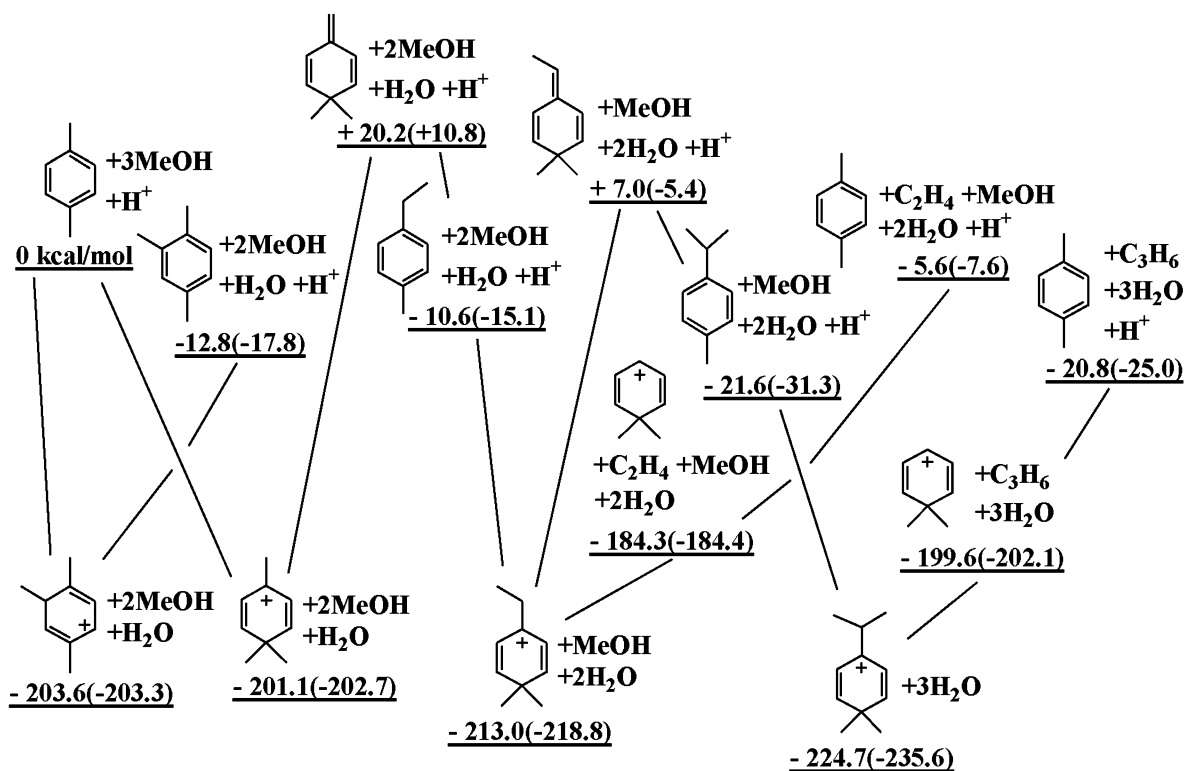


**Figure 1.** Reactants, intermediates, and products from the gas-phase conversion of methanol to ethylene or propene and water on a *p*-xylene reaction center are shown. Enthalpies (relative to starting materials, reported in kcal/mol) shown in the figure were calculated at the B3LYP/cc-pVTZ//B3LYP/6-311G\* and G3(MP2) (in parentheses) levels of theory. Note that the enthalpies of the two intermediates with exocyclic double bonds are significantly reduced at the higher level of theory.

the production of olefins. However, 1,1,4-trimethylbenzenium can only lose a proton from the isolated methyl group, forming an exocyclic double bond. It is this exocyclic double bond that provides the site for side-chain methylation. The result of side-chain methylation is the 1,1-dimethyl-4-ethylbenzenium cation. This species could lose a methyl group to generate 1-ethyl-4-methylbenzene, which does not directly lead to olefins. However, the 1,1-dimethyl-4-ethylbenzenium cation can also undergo an internal hydride shift (the same mechanism presented in detail in our previous study of cyclopentadienyl species as reaction centers<sup>10</sup>) and form ethylene and a 1,1-dimethylbenzenium cation. This secondary benzenium cation would in turn rearrange to the more stable 1,4-dimethylbenzenium cation and then lose a proton to regenerate the *p*-xylene reaction center. Thus, in five primary reaction steps ethylene can be formed.

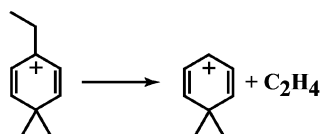
The 1,1-dimethyl-4-ethylbenzenium cation can also lose a proton to regenerate an exocyclic double bond. As before, the exocyclic double bond provides the opportunity for another round of side-chain methylation, giving the 1-isopropyl-4,4-dimethylbenzenium cation. This cation can lose a methyl group to form 1-isopropyl-4-methylbenzene, another step which does not produce olefins. More importantly, the 1,1-dimethyl-4-ethylbenzenium cation can split out propylene via a hydride rearrangement similar to that which produces ethylene, followed by methyl shifts and proton loss to regenerate *p*-xylene. As proposed, propylene production requires two additional primary reaction steps compared to ethylene production.

As noted earlier, the B3LYP/cc-pVTZ//B3LYP/6-311G\* level of theory is not as accurate as we would like for predicting the energetics of the reactions under study. To assess the relative accuracy of the DFT enthalpies we also calculated the relative

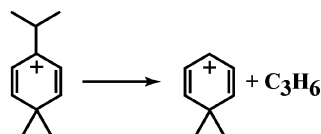
enthalpies for all species in Figure 1 at the G3(MP2) level.<sup>31</sup> The enthalpies shown in plain type for each species in Figure 1 are the B3LYP/cc-pVTZ//B3LYP/6-311G\* values, whereas the G3(MP2) values are given in parentheses. The enthalpies predicted by the two methods differ by ~1–12 kcal/mol, with the G3(MP2) values being generally lower than the B3LYP values relative to starting materials. The intermediate with the highest enthalpy in these schemes is the first exocyclic triene, which is 20.2 kcal/mol above starting materials at the B3LYP/cc-pVTZ//B3LYP/6-311G\* level, but only 10.8 kcal/mol above at G3(MP2). The second exocyclic triene intermediate on the pathway to propene is predicted to be 7.0 kcal/mol uphill from starting materials at the B3LYP/cc-pVTZ//B3LYP/6-311G\* level, whereas it is 5.4 kcal/mol downhill at the more accurate G3(MP2) level.

At the B3LYP/cc-pVTZ//B3LYP/6-311G\* level of theory, the predicted proton affinity of 1,2,4-trimethylbenzene is 190.8 kcal/mol, whereas it is 185.5 kcal/mol at G3(MP2). Although the levels of theory differ between this and previous work, the proton affinity is sufficiently low that the 1,2,4-trimethylbenzenium cation should not be particularly stable in a zeolite. The predicted proton affinity of the first exocyclic species is 221.3 kcal/mol at B3LYP, and 213.5 kcal/mol at G3(MP2). The proton affinity of the second exocyclic species is 220.0 kcal/mol at B3LYP whereas it is 213.4 kcal/mol at the G3(MP2) level. Thus, both the related cations (the 1,1,4-trimethylbenzenium cation and the 1-ethyl-4,4-dimethylbenzenium cations) are predicted to have appreciable lifetimes under reaction conditions.<sup>34</sup> On the basis of these results, we would also predict that the parent olefin of the 1-isopropyl-4,4-dimethylbenzenium cation is sufficiently basic that the cation would be persistent

Scheme 3



Scheme 4



in the zeolite (the G3MP2 proton affinity is 214.3 kcal/mol and the B3LYP/cc-pVTZ//B3LYP/6-311G\* value is 220.3 kcal/mol). The only other cation along the reaction path is 1,1-dimethylbenzenium, and we predict that it should rapidly regenerate the starting *p*-xylene reaction center. As noted earlier, the overall exothermicity of the reactions producing ethylene and propene are well represented by the G3(MP2) method, giving  $-7.6$  and  $-25.0$  kcal/mol compared to experimental values of  $-7.06$  and  $-24.52$  kcal/mol. The B3LYP/cc-pVTZ//B3LYP/6-311G\* level predicts  $-5.6$  and  $-20.8$  kcal/mol for the same reactions.

From the standpoint of catalytic activity and selectivity, the most interesting reaction steps are those leading to release of ethylene (Scheme 3) and propene (Scheme 4). The transition states of these endothermic reactions will more closely resemble the products than the reactants, and we will assume that the relative reaction enthalpies of Scheme 3 and Scheme 4 (or analogous reactions on other reaction centers) will reflect the relative activation barriers. For the specific cases of Schemes 3 and 4 the B3LYP/cc-pVTZ//B3LYP/6-311G\* reaction enthalpies

are 28.7 and 25.1 kcal/mol, respectively. The significance of these and analogous findings are a major topic of the Discussion section.

**Proposed Side-Chain Reaction Mechanism for 1,2,3,5-Tetramethylbenzene.** Figures 2 and 3 show reaction schemes based on 1,2,3,5-tetramethylbenzene reaction centers that differ in whether two of the methyl groups are *ortho* to the departing alkyl groups (Figure 2) or *meta* to those alkyl groups (Figure 3). The gross features of the potential surfaces are similar to each other and to the *p*-xylene mechanism (Figure 1). The reaction mechanisms shown in Figures 2 and 3 were only calculated at the B3LYP/cc-pVTZ//B3LYP/6-311G\* level of theory. Figure 2 shows that two additional methyl groups *ortho* to the departing alkyl group lower the enthalpy of many of the intermediates along the reaction path relative to those with *p*-xylene as the reaction center.

As before, the proton affinities of the parent olefins of the various cations along the reaction pathway should suggest the relative stabilities of the corresponding cations. In this regard, the predicted proton affinity of 6-methylene-1,3,3,5-tetramethylcyclohexa-1,4-diene is 222.5 kcal/mol, whereas the proton affinity of 6-ethylidene-1,3,3,5-dimethylcyclohexa-1,4-diene is 228.1 kcal/mol (Figure 2). Both of these related cations should be persistent in zeolites,<sup>32</sup> lending support to the proposed reaction mechanism. Of the remaining cations in Figure 2, only 1-isopropyl-2,4,4,6-tetramethylbenzenium is capable of losing a proton to form an olefin. The predicted proton affinity of the parent olefin (6-propylidene-1,3,3,5-dimethylcyclohexa-1,4-diene) of this cation is 230.9 kcal/mol.

From Figure 3 we see that methyl group substitution *meta* to the site of side-chain methylation is more effective for stabilizing cation intermediates than the alternative *ortho* positions (Figure

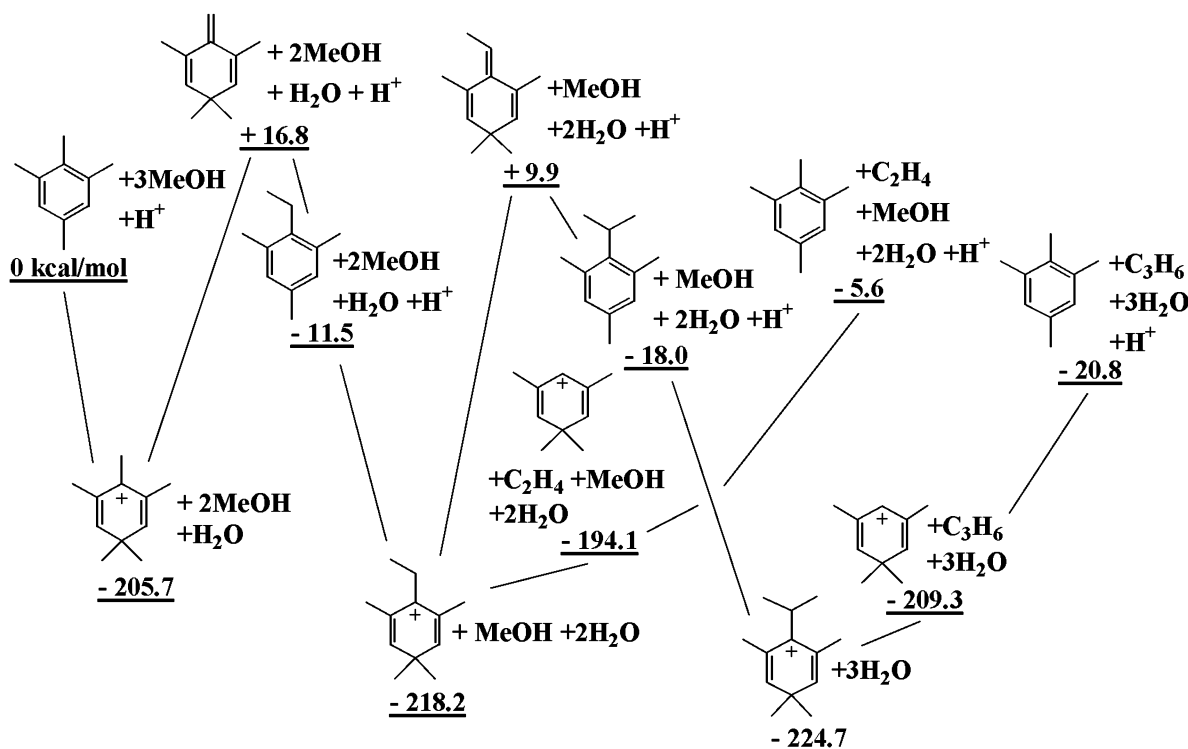


**Figure 2.** Reactants, intermediates, and products from the gas-phase conversion of methanol to ethylene or propene and water on a 1,2,3,5-tetramethylbenzene reaction center are shown for the case where two of the methyl groups are *ortho* to the departing alkyl chain. Enthalpies (relative to starting materials, reported in kcal/mol) shown in the figure were calculated at the B3LYP/cc-pVTZ//B3LYP/6-311G\* level.

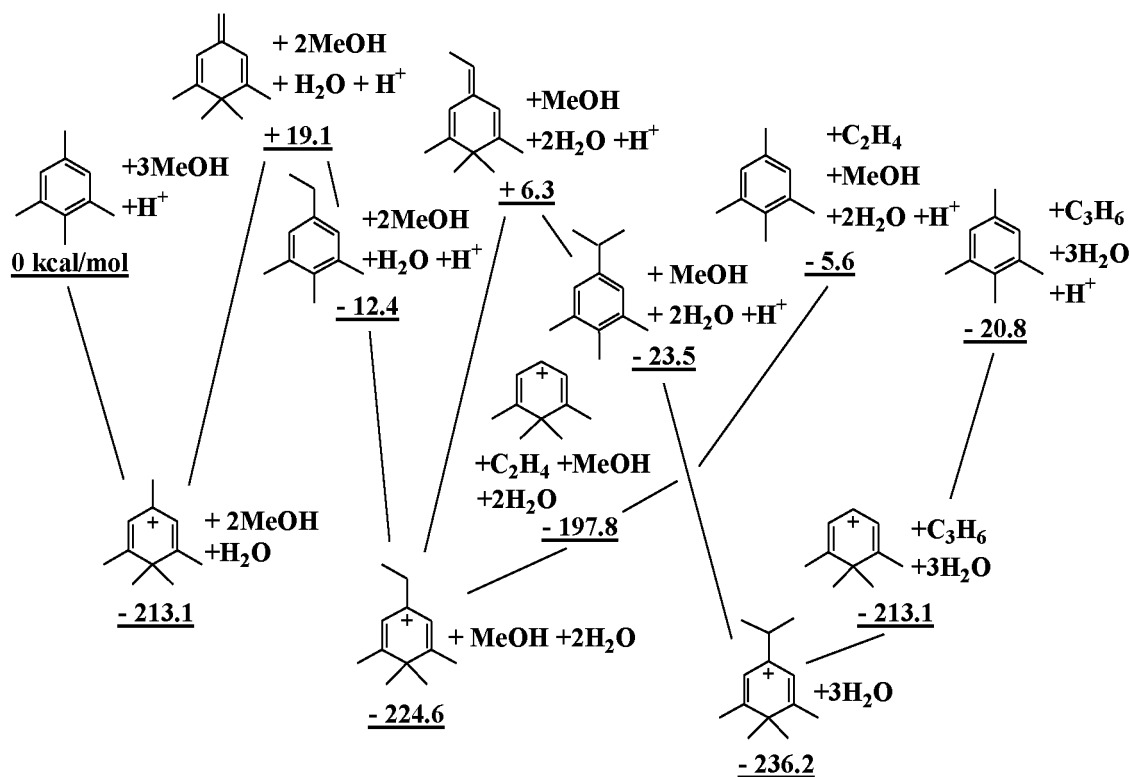


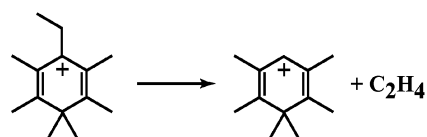
**Figure 3.** Reactants, intermediates, and products from the gas-phase conversion of methanol to ethylene or propene and water on a 1,2,3,5-tetramethylbenzene reaction center are shown for the case where two of the methyl groups are *meta* to the departing alkyl chain. Enthalpies (relative to starting materials, reported in kcal/mol) shown in the figure were calculated at the B3LYP/cc-pVTZ//B3LYP/6-311G\* level.

2). This can be understood by consideration of resonance structures (not shown).

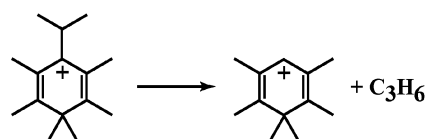
**Proposed Side-Chain Reaction Mechanism for Hexamethylbenzene.** Figure 4 reports the gas-phase reaction mechanism using hexamethylbenzene as the reaction center. Enthalpies are once again calculated at the B3LYP/cc-pVTZ//B3LYP/6-311G\* level of theory only. The gross features are again similar to those of the reaction mechanisms presented earlier. Additional methyl substitution generally lowers the relative energies of the cations.

As before, the intermediate with the highest enthalpy in this mechanism is the first exocyclic triene, with a predicted relative energy of 18.2 kcal/mol above starting materials at the B3LYP/cc-pVTZ//B3LYP/6-311G\* level. The second exocyclic triene intermediate on the pathway to propene is predicted to be 10.6 kcal/mol uphill from starting materials. The predicted proton affinity of the first exocyclic species is 236.0 kcal/mol. The proton affinity of the second exocyclic species is 238.4 kcal/mol. Thus, both related cations (the 1,1,2,3,4,5,6-heptomethylbenzenium cation and the 1-ethyl-2,3,4,4,5,6-hexamethylbenzenium cation) are predicted to have appreciable lifetimes under reaction conditions. The proton affinity of the parent olefin of the 1-isopropyl-2,3,4,4,5,6-hexamethylbenzenium cation is 237.5 kcal/mol at the B3LYP/cc-pVTZ//B3LYP/6-311G\* level. The only other cation along the reaction path is 1,1,2,3,5,6-hexamethylbenzenium, which cannot directly lose a proton to form an olefin. Thus, we again cannot predict its stability on the basis of our previous convention. However, if we consider the methyl rearrangement in addition to proton loss, then this species has a predicted pseudo-proton affinity of 203.8 (or 204.0) kcal/mol. This cation need not be persistent, whereas we predict

#### Scheme 5



#### Scheme 6



that it should rapidly regenerate the starting hexamethylbenzene reaction center.

Schemes 5 and 6 show the reactions leading to the formation of ethylene and propene, respectively, from the hexamethylbenzene-based reaction center. The B3LYP/cc-pVTZ//B3LYP/6-311G\* enthalpies for these reaction steps are 18.2 kcal/mol for formation of ethylene (Scheme 5), but only 9.4 kcal/mol for formation of propene (Scheme 6).

**Hexamethylbenzene and *p*-Xylene Side-Chain Reaction Mechanisms with Zeolite Cluster Model.** As noted earlier, the gas-phase potential surface is notably exaggerated due to the absence of various energetic contributions, particularly those involving proton transfer to and from the zeolite. For the hexamethylbenzene reaction center, and the olefin elimination steps with a *p*-xylene reaction center, we attempted to include these effects by incorporating a zeolite cluster model. The B3LYP/cc-pVTZ//B3LYP/6-311G\* reaction energies for the hexamethylbenzene pathway (not enthalpies in this case) are shown in Figure 5. The most obvious difference between Figures



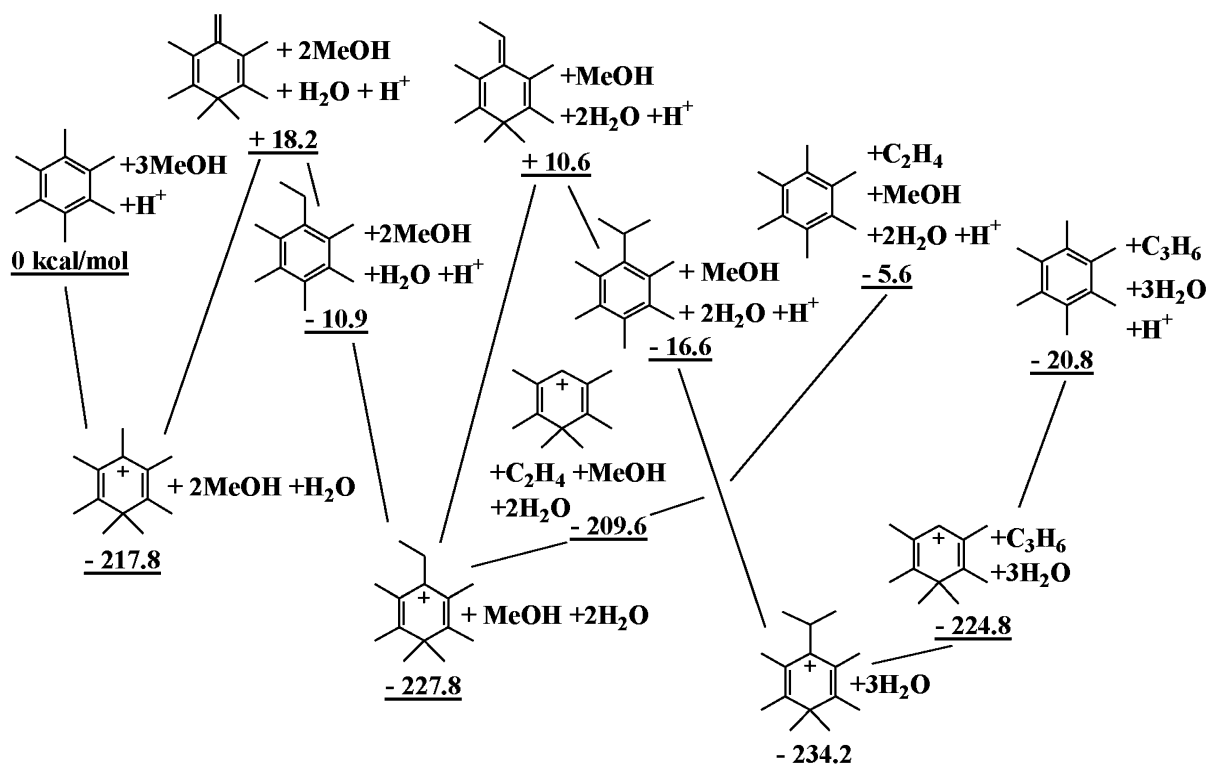


**Figure 4.** Reactants, intermediates, and products from the gas-phase conversion of methanol to ethylene or propene and water on a hexamethylbenzene reaction center are shown. Enthalpies (relative to starting materials, reported in kcal/mol) shown in the figure were calculated at the B3LYP/cc-pVTZ//B3LYP/6-311G\* level.

4 and 5 is that with the inclusion of the zeolite model many of the intermediates are predicted to be higher in energy than starting materials. However, the energies of reaction for Schemes 5 and 6 are little affected by inclusion of the zeolite cluster  $Z^-$ . The specific step forming ethylene has an energy change in Figure 5 of 20.8 kcal/mol and that for forming propene is 10.8 kcal/mol.

In the case of those steps for the *p*-xylene reaction center in the presence of the zeolite cluster corresponding to Scheme 3 (ethylene) and Scheme 4 (propene), the energy differences are 26.4 and 22.5 kcal/mol, respectively.

The geometries of the heptamethylbenzenium cation against the anion of the zeolite cluster as well as the complex of the exocyclic olefin formed by transferring a proton back to the zeolite are shown in Figure 6. The organic molecules are so large that specific interactions with the cluster models are absent. In general, the interatomic distances are greater than 3 Å. For the heptamethylbenzenium cation (Figure 6a) the closest interaction is between the zeolite oxygen and a methyl hydrogen. Interestingly, this proton cannot be readily donated back to the zeolite. Although the hydrocarbons did explore a great deal of conformational space during the optimizations (these complexes are quite “floppy”) it is certainly possible that other minimum energy geometries could be found. Due to the lack of specific interactions, we do not expect that other geometries would afford substantially different energetics. In the complex with the exocyclic olefin (Figure 6b) the closest interaction is between the zeolite acid site proton and one of the methyl protons. However, the acidic proton is pointing toward the exocyclic bond, which we would expect to be the preferred interaction if there was no steric hindrance. The  $\pi$  complex of hexamethylbenzene with the acid site is shown in Figure 6c. In this case

the acidic zeolite proton interacts with the  $\pi$  cloud of the benzene ring, the shortest distance being to one of the benzene carbons. The structures corresponding to the remaining points in Figure 5 are no more or less remarkable than the three shown as representative examples in Figure 6.

## Discussion

**Relationships between Methyl Substituents and Olefin Activity and Selectivity.** In recent experimental work we showed that the activity of methylbenzene reaction centers in HSAPO-34 greatly increases with the average number of methyl groups per benzene ring, as does the propene selectivity.<sup>14</sup> Hexamethylbenzene in HSAPO-34 cages produces olefins at a rate several times that of trimethylbenzenes at a temperature of 673 K. Hexamethylbenzene affords ca. two propenes for every ethylene, but trimethylbenzenes produce nearly equal yields of the two olefins. In related work on the aluminosilicate zeolite HBeta at 723 K, the yield of olefins from hexamethylbenzene was at least five times that of tetramethylbenzene, whereas trimethylbenzenes produced no detectable products.<sup>15</sup> Again, the propene selectivity increased with the number of methyl groups per aromatic ring.

The theoretical calculations presented above strongly support our conclusion that the side-chain mechanism is consistent with two key findings of the experimental work. Table 2 summarizes the B3LYP/cc-pVTZ//B3LYP/6-311G\* enthalpy (or energy) changes for the reactions corresponding to Schemes 3 through 6, with or without inclusion of the zeolite cluster as well as at the G3(MP2) level for Schemes 3 and 4 only. First note that the results in Table 2 support the same general conclusions whether the zeolite cluster is included in the calculation. 1. The



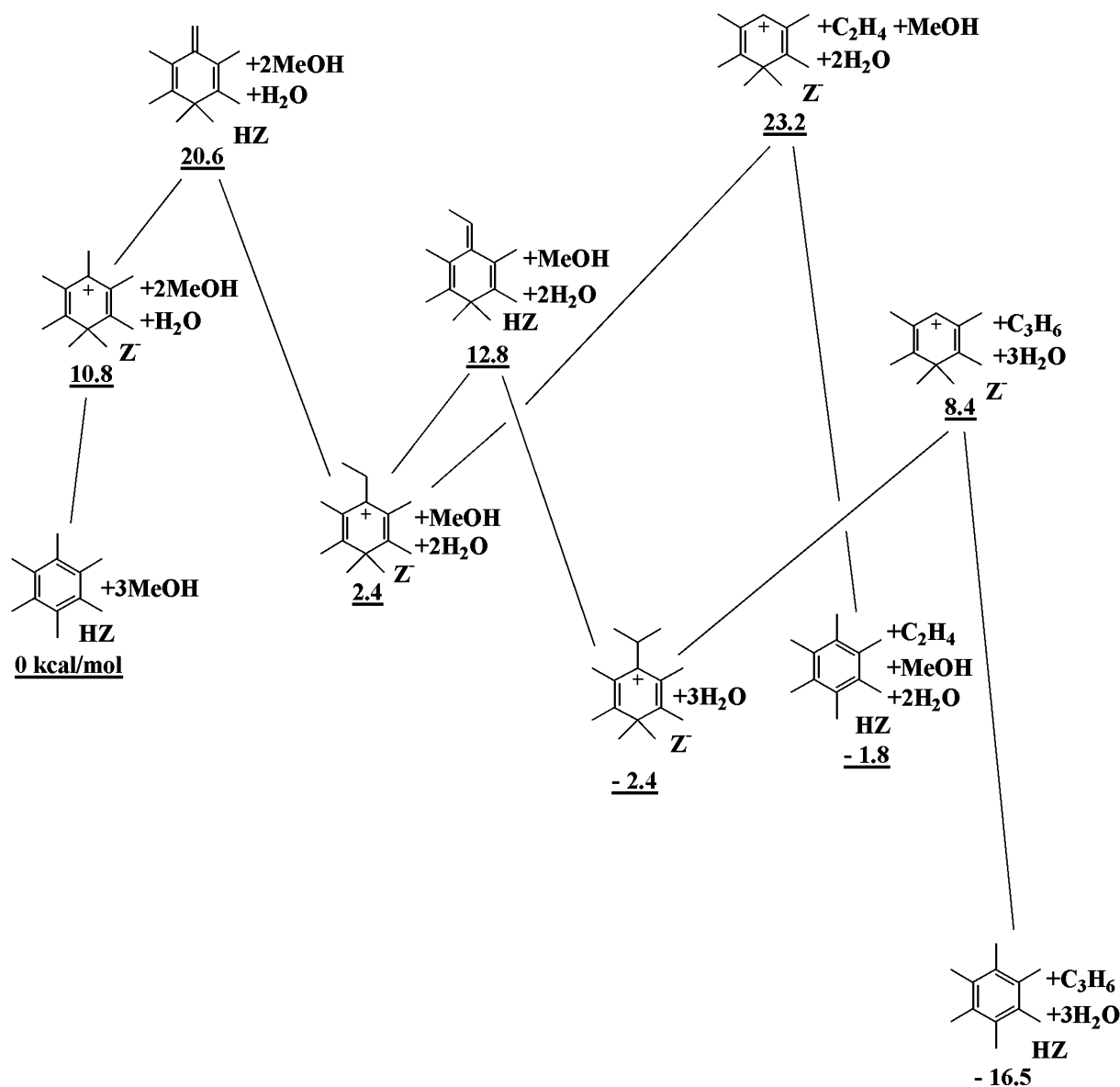


**Figure 5.** Reactants, intermediates, and products for the conversion of methanol to ethylene or propene and water on a hexamethylbenzene reaction center paired with a zeolite cluster model are shown. Each species indicated corresponds to a structure identical or analogous to those in Figure 6. B3LYP/cc-pVTZ//B3LYP/6-311G\* electronic energies rather than enthalpies (as in all other figures) are reported here due to the imaginary frequencies resulting from the imposition of constraints on the zeolite cluster model. Note that inclusion of a cluster model of the zeolite acid site eliminates the deep wells in the potential energy surfaces resulting from the large (gas-phase) proton and methyl cation affinities of aromatics and olefins.

apparent barriers for producing light olefins are substantially reduced by increasing the number of methyl substituents on the methylbenzene reaction center. 2. The selectivity for propene over ethylene as a primary MTO product increases substantially with the number of methyl group substituents.

The intermediate case of four methyl groups per ring is complicated by consideration of two possible mechanisms differing by the positions of the methyl substituents relative to the leaving group, *ortho* (Figure 2) or *meta* (Figure 3). The enthalpies of the reactions analogous to Schemes 3 through 6 are in each case intermediate between the corresponding cases in Table 2, as we would expect. One detail that can be gleaned from a more careful study of the data is afforded by comparison of the enthalpies of the two reactions producing propene; these are 15.4 kcal/mol for the *ortho* case (Figure 2) compared with 23.1 kcal/mol for the *meta* case (Figure 3). Our interpretation of this difference is that steric repulsion between the isopropyl

group and adjacent methyl substituents destabilizes the reactant and hence lowers the apparent barrier to propene elimination. Note that the corresponding reactions forming ethylene in Figures 2 and 3 have very similar enthalpy changes, consistent with our steric argument.

**Theoretical Methodology versus Real Catalysis.** DFT methods are very commonly used to model reaction pathways in heterogeneous and homogeneous catalysis, and we do not question the fact that they are generally useful for such. The limitations of DFT for the thermochemical values of nonisodesmic reactions have been noted previously, but we were nonetheless surprised by the magnitude of the errors in the reaction enthalpies for the conversion of methanol to ethylene or propene and water with the commonly used 6-311G\* basis sets. Fortunately, these deficiencies are largely eliminated through single-point corrections using the cc-pVTZ basis sets modified to include diffuse functions on oxygen.

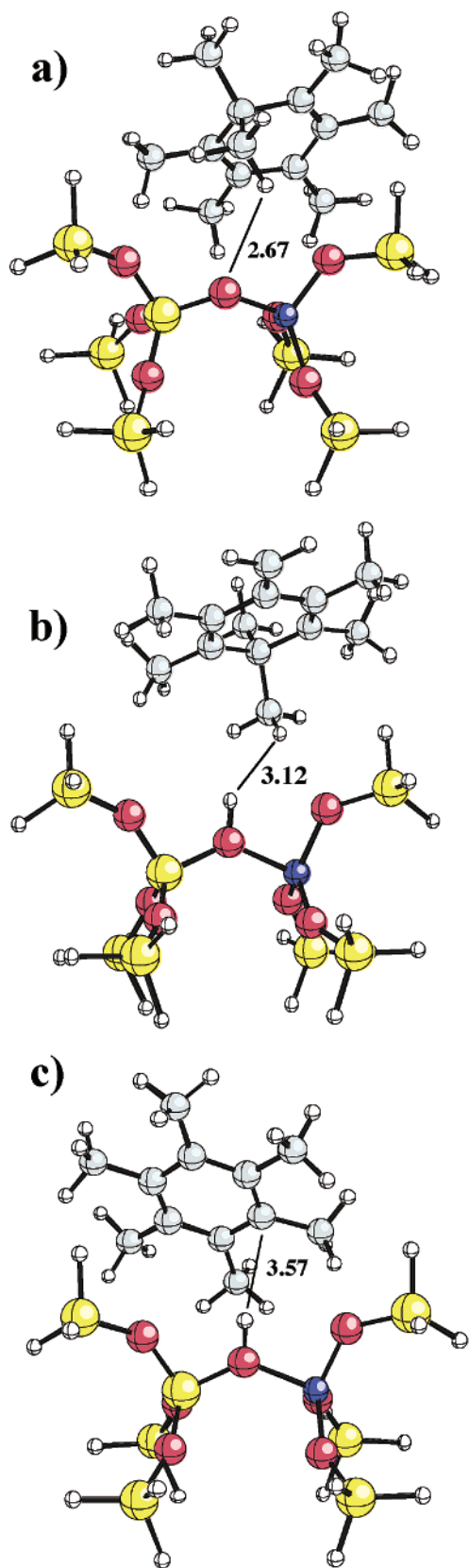


**Figure 6.** B3LYP/6-311G\* geometries of three of the species modeled in the conversion of methanol to ethylene or propene on water on a hexamethylbenzene reaction center in contact with a zeolite cluster model. Selected distances in Å are shown. (a) The heptamethylbenzenium cation paired with the anion of the zeolite cluster model. (b) The complex of the acid site cluster with the neutral olefin with an exocyclic double bond. (c) The complex of the acid site cluster model with hexamethylbenzene.

**Table 2.** Energetics of Olefin Elimination from Various Reaction Centers

reaction (scheme)	product	$\Delta H_{G3(MP2)}$ (kcal/mol)	$\Delta H_{B3LYP}$ (kcal/mol)	$\Delta E_{B3LYP}$ on $Z^-$ (kcal/mol)
3	ethylene	34.4	28.7	26.4
4	propene	33.5	25.1	22.5
5	ethylene		18.2	20.8
6	propene		9.4	10.8

Unfortunately, our computer resources were insufficient to apply G3(MP2) theory to structures including cluster models of the zeolite, and even repeating the gas-phase schemes in Figures 3–6 at G3(MP2) would be expensive if technically possible. Thus, our overall view of the reaction mechanism is shaped here through a heavy reliance on B3LYP/cc-pVTZ//B3LYP/6-311G\* calculations after carefully understanding their limitations by judicious application of G3(MP2) theory (i.e., Figure 1).

We computed enthalpies for isolated species rather than clusters of reactants, intermediates, and/or products. For example, our starting points could have been optimized gas-phase clusters of a methylbenzene molecule and three methanol molecules, with the proton still at infinite distance, and our final products could have been ensembles of propene, three waters, and methylbenzenes. This point is largely aesthetic, and the overall enthalpy differences with this omission would not alter our conclusions. A larger limitation is our omission of transition state calculations, which was purely a consequence of their difficulty. We presented these previously for a closely analogous scheme based on dimethylcyclopentenyl reaction centers. The most important reactions in Figures 1–5 are elimination of ethylene or propene; these are endothermic reactions for which the transition states will be product-like. Thus, we expect the values of reaction enthalpies for these steps to be qualitatively predictive of relative rates for forming ethylene or propene when compared with each other.

Methanol to hydrocarbon catalysis has been performed industrially on at least two very different types of catalysts, and it has been investigated by researchers using a wide variety of materials.<sup>4</sup> Historically, most interest was centered on the aluminosilicate zeolite HZSM-5,<sup>2</sup> either without modification or sometimes with included inorganic matter to limit the secondary reactions of olefins to aromatics and alkanes. The products obtained from unmodified HZSM-5 include one isomer of tetramethylbenzene, and in situ NMR has shown the formation of a pentamethylbenzenium cation,<sup>19</sup> but there may not be sufficient room in the channels for formation of either hexamethylbenzene or the heptamethylbenzenium cation as modeled in Figures 5 and 6. These species have however been studied in the 12-ring aluminosilicate HBeta, which is not a practical methanol conversion catalyst as a result of product selectivity and rapid deactivation. A second type of methanol conversion catalyst that has attracted commercial interest is exemplified by the silico-aluminophosphate HSAPO-34.<sup>35</sup> The acid sites in this material are Si–OH–Al groups imbedded in an aluminophosphate framework, and they are believed to be weaker in strength than those in the aluminosilicate cluster model used in our work. The CHA topology of HSAPO-34

(35) Wilson, S.; Barger, P. *Microporous Mesoporous Mater.* **1999**, *29*, 117–126.

features cages of ca. 1 nm size that readily hold hexamethylbenzene molecules with additional room for methanol and product molecules.

It goes without saying that our limited efforts to model the catalyst using a small, if established, cluster model based on a fragment of the HZSM-5 structure neglects essentially all topological constraints. The present study found some evidence that steric constraints within a gas-phase reaction center contribute to propene/ethylene selectivity. We would not be surprised if the catalyst topology was capable of amplifying such effects. Quantum chemical periodic electronic structure calculations provide an efficient way to describe the interactions between the guest molecules and the zeolite framework. Several studies along these lines have been carried out for various hydrocarbon reactions in the zeolite framework including methylation of toluene,<sup>36</sup> isomerization reactions of toluene and xylenes,<sup>37</sup> cracking reactions,<sup>38</sup> chemisorption of propene and isobutene in zeolite frameworks,<sup>39,40</sup> isomerization of 2-pentene,<sup>41</sup> and hydride transfer reactions.<sup>42</sup> As an alternative or

adjunct to periodic calculations, QM/MM embedding studies can also be done to include the zeolite topology in theoretical descriptions of hydrocarbon reactions in zeolites.<sup>43</sup> Similar approaches would be required for more detailed future extensions of the present investigation.

## Conclusions

Limitations aside, the present investigation has established that the methylbenzene side-chain hydrocarbon pool route is plausible in MTO catalysis. The enthalpies of the intermediates are not excessive, and there are no deep valleys in the potential surface when a cluster model is used to include the catalyst. Most importantly our theoretical calculations reproduce the essential experimental observations that activity of a methylbenzene reaction center increases with the number of methyl substituents as does its selectivity for propene compared to ethylene as primary hydrocarbon products.

**Acknowledgment.** This work was supported by the National Science Foundation (CHE-020539). Bjørnar Arstad would like to acknowledge the Norwegian research Council for financial support through grant 135867/431, and a grant of computer time through the NOTUR project (account No. NN2878K).

JA035923J

- (36) Vos, A. M.; Rozanska, X.; Schoonheydt, R. A.; van Santen, R. A.; Hutschka, F.; Hafner, J. *J. Am. Chem. Soc.* **2001**, *123*, 2799–2809.  
(37) Rozanska, X.; van Santen, R. A.; Hutschka, F.; Hafner, J. *J. Am. Chem. Soc.* **2001**, *123*, 7655–7667.  
(38) Rozanska, X.; van Santen, R. A.; Hutschka, F.; Hafner, J. *J. Catal.* **2003**, *215*, 20–29.  
(39) Rozanska, X.; Demuth, T.; Hutschka, F.; Hafner, J.; van Santen, R. A. *J. Phys. Chem. B* **2002**, *106*, 3248–3254.  
(40) Rozanska, X.; van Santen, R. A.; Demuth, T.; Hutschka, F.; Hafner, J. *J. Phys. Chem. B* **2003**, *107*, 1309–1315.  
(41) Demuth, T.; Rozanska, X.; Benco, L.; Hafner, J.; van Santen, R. A.; Touhoat, H. *J. Catal.* **2003**, *214*, 68–77.

- (42) Boronat, M.; Zicovich-Wilson, C. M.; Corma, A.; Viruela, P. *Phys. Chem. Chem. Phys.* **1999**, *1*, 537–543.  
(43) Clark, L. A.; Sierka, M.; Sauer, J. *J. Am. Chem. Soc.* **2003**, *125*, 2136–2141.